ISSN 1674-1056
http://cpb.iphy.ac.cn
http://iopscience.iop.org/cpb
中国物理 B
Chinese Physics
中国物理
Chinese Physics B

## Topology and ferroelectricity in group-V monolayers

Mutee Ur Rehman, Chenqiang Hua(华陈强), Yunhao Lu(陆赟豪)
**Citation:**Chin. Phys. B . 2020, 29(5): 057304 . **doi:** 10.1088/1674-1056/ab81ff
Journal homepage: http://cpb.iphy.ac.cn; http://iopscience.iop.org/cpb

**What follows is a list of articles you may be interested in**

---

## Recent progress on the prediction of two-dimensional materials using CALYPSO

Cheng Tang(唐程), Gurpreet Kour, Aijun Du(杜爱军)
Chin. Phys. B . 2019, 28(10): 107306 . **doi:** 10.1088/1674-1056/ab41ea

## Emerging properties of two-dimensional twisted bilayer materials

Yang Cheng(程阳), Chen Huang(黄琛), Hao Hong(洪浩), Zixun Zhao(赵子荀), Kaihui Liu(刘开辉)
Chin. Phys. B . 2019, 28(10): 107304 . **doi:** 10.1088/1674-1056/ab3e46

## Room-temperature infrared photodetectors with hybrid structure based on two-dimensional materials

Tiande Liu(刘天德), Lei Tong(童磊), Xinyu Huang(黄鑫宇), Lei Ye(叶镭)
Chin. Phys. B . 2019, 28(1): 017302 . **doi:** 10.1088/1674-1056/28/1/017302

## Strain-induced insulator-metal transition in ferroelectric $BaTiO_3$ (001) surface: First-principles study

Lin Yang(杨林), Chang-An Wang(王长安), Cong Liu(刘聪), Ming-Hui Qin(秦明辉), Xu-Bing Lu(陆旭兵), Xing-Sen Gao(高兴森), Min Zeng(曾敏), Jun-Ming Liu(刘俊明)
Chin. Phys. B . 2016, 25(7): 077302 . **doi:** 10.1088/1674-1056/25/7/077302

## Coupling-matrix approach to the Chern number calculation in disordered systems

Zhang Yi-Fu, Yang Yun-You, Ju Yan, Sheng Li, Shen Rui, Sheng Dong-Ning, Xing Ding-Yu
Chin. Phys. B . 2013, 22(11): 117312 . **doi:** 10.1088/1674-1056/22/11/117312

---

TOPICAL REVIEW — Topological 2D materials

# Topology and ferroelectricity in group-V monolayers*

Mutee Ur Rehman[1,†], Chenqiang Hua(华陈强)[1,2,†], and Yunhao Lu(陆赟豪)[1,2,‡]

[1] State Key Laboratory of Silicon Materials, School of Materials Science and Engineering, Zhejiang University, Hangzhou 310027, China
[2] Zhejiang Province Key Laboratory of Quantum Technology and Device, Department of Physics, Zhejiang University, Hangzhou 310027, China

(Received 31 December 2019; revised manuscript received 19 February 2020; accepted manuscript online 23 March 2020)

The group-V monolayers (MLs) have been studied intensively after the experimental fabrication of two-dimensional (2D) graphene and black phosphorus. The observation of novel quantum phenomena, such as quantum spin Hall effect and ferroelectricity in group-V elemental layers, has attracted tremendous attention because of the novel physics and promising applications for nanoelectronics in the 2D limit. In this review, we comprehensively review recent research progress in engineering of topology and ferroelectricity, and several effective methods to control the quantum phase transition are discussed. We then introduce the coupling between topological orders and ferroelectric orders. The research directions and outlooks are discussed at the end of the perspective. It is expected that the comprehensive overview of topology and ferroelectricity in 2D group-V materials can provide guidelines for researchers in the area and inspire further explorations of interplay between multiple quantum phenomena in low-dimensional systems.

**Keywords:** topology, ferroelectricity, two-dimensional material, group-V element

**PACS:** 73.43.–f, 77.80.–e, 03.65.–w, 31.15.em **DOI:** 10.1088/1674-1056/ab81ff

## 1. Introduction

Two-dimensional (2D) materials have revolutionized the new generation of devices. Decreasing the thickness of materials down to single (or several) atomic layer has attracted tremendous interest since they could display exotic phenomena which are different from their bulk counterparts, e.g., quantum spin Hall effect,[1–4] 2D ferroelectricity,[5] superconductivity,[6–8] or magnetism.[9–11] Motivated by the remarkable progress of graphene,[12,13] 2D materials other than graphene have been a pronounced research field of interest. Recent experimental successes in the elemental 2D layers have invigorated the search for more fascinating structures and properties based on elemental 2D systems, for example, Si (silicene),[14–16] Ge (germanene),[17,18] Sn (stanene),[19] B (borophene),[20] P (phosphorene),[21] As (arsenene),[22] Sb (antimonene),[23] Bi (bismuthene),[4] Te (tellurene),[24] and Se (selenene).[25]

Graphene, the first successfully isolated elemental material in 2D limit with the honeycomb lattice, holds the linear band dispersion and crossing at the $K$ point in the 1$^{st}$ Brillouin zone (BZ), generating the Dirac fermions. Actually, a tiny energy gap opens up at the Dirac points due to spin–orbital coupling (SOC) and graphene is a quantum spin Hall (QSH) insulator.[26] QSH insulators, also named as 2D topological insulators (TI), hold counter-propagating and oppositely spin-polarized conducting states at their edges, which are protected by the time reversal symmetry against the weak localized perturbations. Therefore, these robust edge states endow 2D TIs with possibilities for a wide range of applications in dissipationless electronics, topological quantum computing, and so on.[27–30] However, the SOC effect in graphene is too small to achieve the experimental measurement and topological electronic devices,[31] which stimulates scientists to search for large-gap 2D TIs not only in compounds but also in elemental materials. For example, graphene-like honeycomb structures have been widely explored including group-IV and group-V materials.[32,33] For group-V materials, except for the graphene-like structures, the puckered structures in black phosphorus lattice are also able to exhibit topological properties.[34] This puckered structure is unique for group-V elements due to the one extra valence electron compared to group-IV elements and provides a feasible way to tune the crystal symmetry and distortion of the 2D system, allowing intimate coupling and control between various order parameters.

Ferroelectricity is also an exciting ferroic order, possessing reversible spontaneous electronic polarization which is important for applications in non-volatile memory devices, field effect transistors, solar cells, and sensors.[35–38] Normally, ferroelectricity would disappear when the film thickness is below a critical value, due to the depolarizing electric field and electron screening. A new class of materials, called as hyperferroelectrics, have been identified to remain in stable po-

*Project supported by the National Natural Science Foundation of China (Grant Nos. 11974307 and 61574123), Zhejiang Provincial Natural Science Foundation, China (Grant No. D19A040001), the Fundamental Research Funds for the Central Universities of China, and the 2DMOST, Shenzhen University (Grant No. 2018028).

†These authors contributed equally to this work.
‡Corresponding author. E-mail: luyh@zju.edu.cn

© 2020 Chinese Physical Society and IOP Publishing Ltd 

lar states in ultrathin atomic layers against unscreened depolarizing field.[39] However, the experimental evidence of these materials is still rare. Recently, the ferroelectric instability becomes of interest in 2D van der Waals materials[40,41] and 2D ferroelectricity is identified in 2D group-V binary compounds[42] and elemental monolayers (MLs),[43] which is impossible for their 3D bulk counterparts. Conventionally, the intrinsic ferroelectricity has been reported only for compounds in which the required positive and negative charge centers are carried by different elements. The elemental materials are always stable in centrosymmetric structures without intrinsic ferroelectricity. While, the lack of constrain in one dimension could break the inversion symmetry and drive the 2D elemental layers into a ferroelectric state.[43–45]

The coupling between different ordering parameters is important not only for fundamental research, but also meaningful for cross-control of different orderings in applications. The most striking of such controls is switching magnetic ordering and/or ferroelectric polarization ordering (referred as multiferroicity or magnetoelectric coupling) by electric and magnetic fields, which is important for the design of new electronic devices.[46,47] There are a lot of work and reviews discussing coupling between magnetic and electronic orderings. As far as we know, there is still no review touching interplay between electronic topological ordering and ferroelectric polarization/charge ordering in 2D materials. In this paper, we will systematically report the recent advances about the topology and ferroelectricity in group-V 2D materials. Starting from structure classification of group-V MLs, we will summarize the recent work on 2D group-V MLs about the topology and ferroelectricity with their possible approaches of modulation (e.g., electric field, chemical functionalization, and fabricating the binary systems). Lastly, we would like to discuss the possible coupling between these two interesting quantum properties. Here, the topology refers to the electronic structure, not the topological domain pattern in ferroelectric materials that is the topology of the geometrical structure. We certainly do not make any attempt to cover everything in this mini-review, and the topics chosen are more or less biased by the author's own research interests. The review mainly focuses on group-V MLs and only the advances in the last several years will be discussed.

## 2. Structural allotropes

### 2.1. Bulk allotropes

Before the discussion of 2D layers, we firstly discuss the structure character of bulk group-V elements. There are five valence electrons in group-V elements and diverse valence states ($-3$, $+3$, and $+5$) are possible for them, resulting in a variety of structural allotropes for bulk of group-V elements at ambient conditions. Phosphorus, the most studied element of group-V, has several allotropes, which are named as white, red, blue, violet, and black phosphorus.[48–51] In addition, amorphous phosphorus is also very popular.[51,52] The discovery of black phosphorus, the most stable allotrope of phosphorus at ambient conditions, is dated back in 1914[50,53] and it crystallizes in parallel puckered layer orthorhombic structure with space group *Cmca* as shown in Fig. 1(a). The 3s and 3p orbitals of phosphorus undergo $sp^3$ hybridization in a tetrahedral geometry to form three $\sigma$-covalent bonds along with an out-of-plane oriented lone pair of electrons. Two of these three covalent bonds lie parallel to the plane while the third one is almost perpendicular to the plane, forming a puckered layer. And, the out-of-plane lone pair electrons combine the puckered layers together, crystalizing in the orthorhombic structure ($\alpha$ phase). Phosphorus can also crystallize into a rhombohedral geometry, i.e., blue phosphorus ($\beta$ phase) with space group $R\bar{3}m$.[54] Blue phosphorus also adopts a layered structure with buckled layers consisting of knitted honeycomb rings as shown in Fig. 1(b), where the three $\sigma$-covalent bonds within the layer are equivalent, resulting in the hexagonal structure.

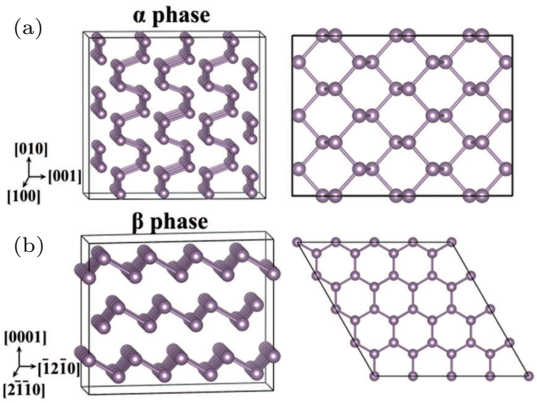



**Fig. 1.** Two typical stable phases of group-V elements: (a) orthorhombic $\alpha$ phase with space group *Cmca*, and (b) rhombohedral $\beta$ phase with space group $R\bar{3}m$. Left and right panels show side and top views, respectively.

Although the most stable crystal structure of phosphorus is the $\alpha$ phase with orthorhombic space group, the other elements of group-V (As, Sb, and Bi) favor the $\beta$ phase due to the weak s–p hybridization.[55,56] The delocalized p–p coupling causes more and more metallic bonding between atoms from As, Sb to Bi and the hexagonal honeycomb structure becomes more stable. For example, the most common and stable allotrope of As and Sb has the rhombohedral layered structure with space group $R\bar{3}m$ as shown in Fig. 1(b), consisting of two interpenetrating, face-centered-cubic lattices which are displaced in the [111] direction and slightly distorted in the [111] direction. While the $\alpha$ phase is a metastable phase, the phase transformation between $\beta$ and $\alpha$ is observed for both As and Sb.[57] For bulk Bi, the last element of group-V, only the

rhombohedral structure ($\beta$ phase) has been observed in experiment.

### 2.2. Two-dimensional allotropes

Generally, there are more crystal allotropes for 2D materials than the corresponding 3D ones due to the lack of periodic boundary constrain along one dimension. For 2D group-V layers, a lot of allotropes have been predicted by theoretical calculations,[58–61] as shown in Fig. 2(a). Although several phases could be found under unique experimental conditions,[48] the $\alpha$ and $\beta$ phases are more stable than the others (Fig. 2(b)), which can be viewed as single layers cleaved from the bulk (Fig. 3(a)). For example, $\alpha$-P (black phosphorene) ML has already been exfoliated from bulk $\alpha$ phase along [001] direction[62] and $\beta$-P (blue phosphorene) ML can be grown along [0001] direction of bulk $\beta$ phase by chemical vapor deposition (CVD).[63] Both $\alpha$ and $\beta$ group-V films have been experimentally obtained,[64–68] although the experimental evidence of $\beta$-P ML is still under debate.[69,70] Their dynamic stability has also been confirmed through phonon spectra as shown in Fig. 3(b), without any appreciable imaginary modes. In fact, most of group-V layers fabricated in experiment are $\alpha$ and $\beta$ phases.[4,21,71–73] These two phases are more popular and observed in experiment for all group-V elements.[74] Thus, we only focus on these two phases in the following.

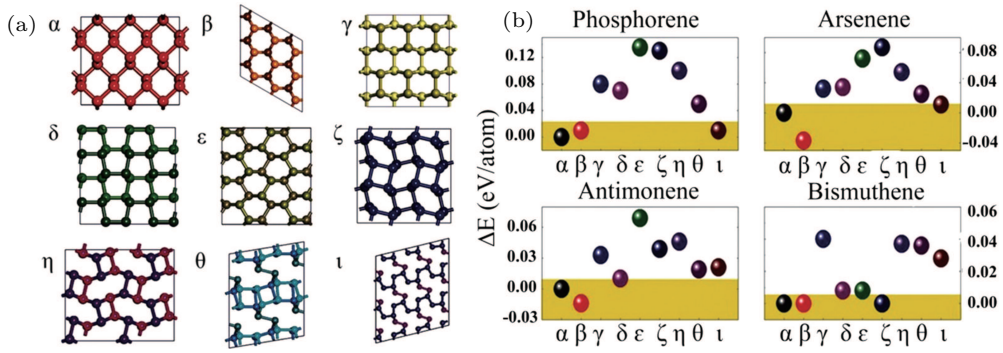



**Fig. 2.** (a) Top views of 9 group-V ML allotropes with five typical honeycomb structures ($\alpha$, $\beta$, $\gamma$, $\delta$, $\varepsilon$) and four non-honeycomb structures ($\zeta$, $\eta$, $\theta$, $\iota$). (b) Comparison of stabilities in terms of energies for different allotropes of group-V MLs.[59]

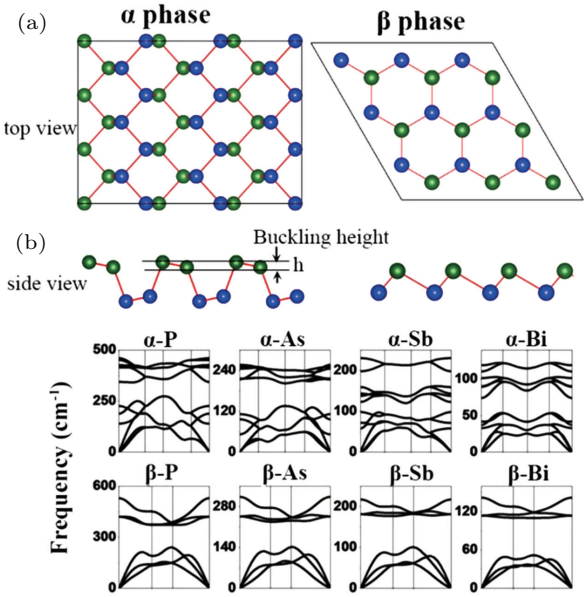



**Fig. 3.** (a) Top view and side view of $\alpha$ and $\beta$ phases with two atomic layers (green and blue). The buckling height $h$ is marked for $\alpha$ phase. When $h$ is non-zero, the inversion symmetry of the structure breaks. (b) Phonon dispersions of group-VA MLs in $\alpha$ and $\beta$ phases.[59]

For the $\beta$ phase, all group-V MLs have buckled honeycomb lattices with two atomic layers, the same as silicene, which are not in the same plane due to the special valence electrons ($s^2p^3$) and mixed $sp^3$ hybridization. There is buckling difference for different group-V MLs, but the space group (symmetry) is the same for all of them. For the $\alpha$ phase, all group-V MLs take the puckered lattice with orthogonal structure and there is also buckling difference (Fig. 3(a)) for different group-V MLs, e.g., the buckling height ($h$) of $\alpha$-P is zero and that of $\alpha$-Bi varies from zero to nonzero. Importantly, this nonzero buckling breaks the inversion symmetry of the $\alpha$ phase, quite different from the buckling in the $\beta$ phase, and largely correlates to the topological and ferroelectric properties of the $\alpha$ phase, which will be discussed below.

## 3. Quantum spin Hall effect in 2D group-V monolayer

Topological insulators, as a new quantum state of matter, have attracted intensive research interest due to their applications in spintronics and topological quantum computation as well as academic importance as a novel quantum phenomenon.[75,76] Actually, topological properties in 3D group-V have attracted attention for more than ten years. The valence band of bulk Sb is equivalent to that of a strong topological insulator and bulk Bi is a conventional insulator due to the band inversion at $L$ point. Both bulk Bi and Sb are semimetal with electron and hole pockets at different $K$ points. Since they both have the rhombohedral structure, the Bi–Sb alloy is introduced to open a global bandgap in BZ and maintains the nontrival character.[77]

Two-dimensional TIs also named as QSH insulators are

considered as more valuable than 3D TIs for spin transport applications, because the edge states in the former are more robust against back-scattering caused by non-magnetic defects than the surface states in the latter. QSH insulators possess edge states protected by the time reversal symmetry. As stated above, graphene was the first predicted QSH insulator. But, due to the lack of strong SOC, it is difficult to open up a bandgap for experimental observation in graphene. The 2D MLs of group-V elements (P, As, Sb, and Bi) are considered as new emerging 2D materials with much stronger SOC effect than graphene. Moreover, there are diversified ways to tune the topological character of 2D MLs of group-V elements and the cross-control of quantum states may be more easily accessed in the 2D systems. Therefore, as new members in the 2D material family, they can be potential candidates to study the QSH effect under appropriate conditions.

### 3.1. The $\alpha$ phase monolayer

Firstly, we discuss the $\alpha$ phase without buckling ($h = 0$ in Fig. 3(a)). In the inversion symmetric $\alpha$ phase, the structure has a non-symmorphic $D_{2h}$ (7) space group with two sublattices (A and B in Fig. 4(a)). Based on the tight-binding model, two types of Dirac fermions have been predicted in the 1st BZ as shown in Figs. 4(b) and 4(c).[78] A pair of type-I Dirac points locate along $\Gamma$–$X_2$ and are mainly determined by the $p_z$ orbital (Fig. 4(c)) between the two atomic layers, which are very sensitive to the interaction or distance between the layers. There are four type-II Dirac points protected by mirror symmetry, so that they carry opposite Chern numbers and appear in pairs (Fig. 4(b)). Type-II Dirac points are mainly determined by the $p_x$ orbital (Fig. 4(d)) and sensitive to the in-plane strain. When a strain is applied, type I Dirac points only move along $\Gamma$–$X_2$ line while type II points are located at generic $k$-points. Thus, the $\alpha$ phase without buckling could hold six Dirac points in the 1st BZ, like graphene, although their space groups are different. The main difference is that the Dirac points in $\alpha$ phase can move in BZ without changing symmetry while they are pinned at $K$ points in graphene. Therefore, a QSH insulator with large topological gap can also be realized in $\alpha$ phase, although a strain or external field may be needed for the phase transition. For example, intrinsic $\alpha$-P is a normal insulator with a bandgap around $\Gamma$ point and a large strain ($\sim$ 16%) along the zigzag direction is needed for the emergence of type-II Dirac points. While, only 6% strain is needed for the phase transition of $\alpha$-As.[79] Besides the strain modulation, application of electric field is also proposed to tune the bandgap and create the type-I Dirac points. In Fig. 5, an electric field (0.3 V/Å) perpendicular to the 2D plane is applied to close the bandgap of 4 ML $\alpha$-P and causes the topological phase transition (0.55 V/Å for 3 ML).[80] Adsorption of alkali atom on the surface of $\alpha$-P has similar effect as electric field and Dirac states have been observed in experiment by surface doping of potassium.[81] The structure parameters and electronic coupling between atoms of other group-V elements are different from those of $\alpha$-P and the critical values for the topological phase transition are also different. Especially, the interlayer coupling of $\alpha$-Bi is already weak enough and it is an intrinsic non-trivial 2D TI with large SOC gap[78] (gapped type-I Dirac points as aforementioned). More importantly, the large-scale growth of $\alpha$-Bi has been realized[65] and the evidence of topological edge state along the edge of $\alpha$-Bi has also been observed in experiment.[73] Thus, $\alpha$-Bi is a good elemental 2D material with intrinsic topological properties to investigate different kinds of quantum states controlled by thickness, gating, and substrate interaction. Very recently, $\alpha$-Sb has been successfully grown on $T_d$-$WTe_2$ substrate[74] and another experimental work claimed that 2 ML or 4 ML $\alpha$-Sb becomes non-trivial due to the layer stacking.[82]

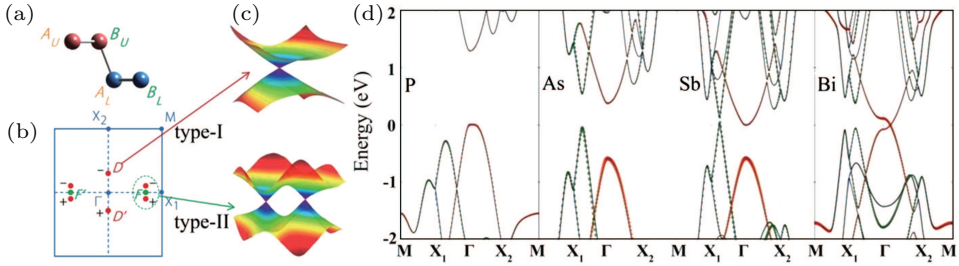



**Fig. 4.** (a) Basis sites in a unit cell of centrosymmetric puckered $\alpha$ structure. (b) 2D rectangular BZ with Dirac points marked by red dots. A pair of type-I Dirac points are marked as $D$ and $D'$ on $\Gamma$–$X_2$, while two pairs of type-II Dirac points are marked (red dots) near $F$ and $F'$ on $\Gamma$–$X_1$. (c) Schematic energy dispersions around $D$ and $F$ points respectively illustrating type-I and type-II Dirac points. (d) Band structures of 2D phosphorene ($\alpha$ phase with $h = 0$) type lattice structure of group-V elements in the absence of SOC, the red and green dots size shows the projection on the $p_z$ ($p_x$) atomic orbitals.[78]

As mentioned above, the atomic buckling in $\alpha$ phase is related to the inversion symmetry and quite important for topological properties. Except for $\alpha$-P, the atomic buckling ($h$) of other group-V elements could be nonzero and different from each other due to different hybridization between two atomic layers or substrate effect. This buckling breaks the inversion symmetry and degeneracy of crossing points, and even causes the topological phase transition. This effect is most remarkable in $\alpha$-Bi. Because of the negligible s–p hybridization and the formation of lone pair,[43] the spontaneous buckling

height of $\alpha$-Bi can vary in a wide range (0.0–0.5 Å). The different buckling height results in different $p_z$ interaction and thus changes the topological gap. The non-trivial QSH effect (phase transition) is determined by atomic buckling ($h$), as shown in Fig. 6.[73] The $\alpha$-Bi is topologically non-trivial at low buckling heights (e.g., $h < 0.1$ Å ) and transforms to trivial insulator when $h$ is large enough. Normally, atomic buckling is sensitive to charge ordering or charge transfer between substrate and epitaxial film. Thus, this buckling-dependent QSH effect provides a unique way to control the topological character at atomic level and very helpful for the design of topological device.

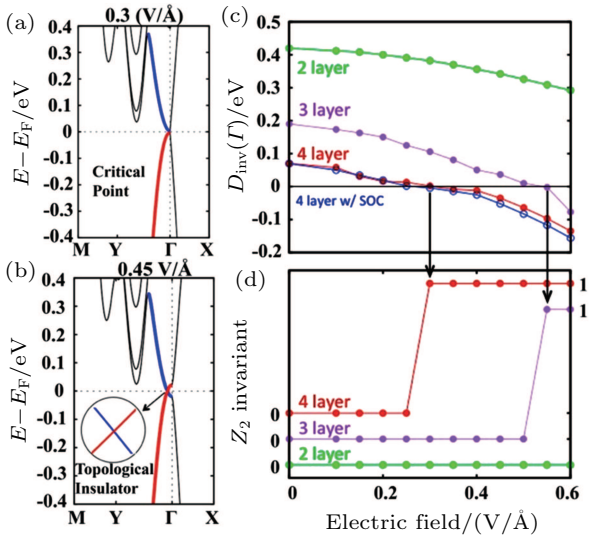



**Fig. 5.** (a) Band structure of phosphorene layers (4 L) with applied external electric field of (a) 0.3 V/Å and (b) 0.45 V/Å without including SOC. The red and blue lines show the top valence and bottom conduction states, respectively. (c) Inversion energy $\Delta_{inv}$ and (d) $Z_2$ invariant of 2-, 3-, and 4-layer phosphorene as a function of electric field. The negative values of $\Delta_{inv}$ show non-trivial topological phases. It can be seen that the phase transition takes place for 3- and 4-layer phosphorene at a critical field of 0.55 V/Å and 0.3 V/Å, respectively.[80]

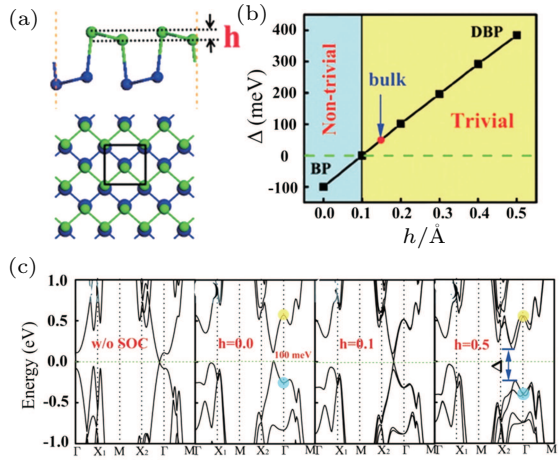



**Fig. 6.** (a) Side and top views of $\alpha$-Bi ML with buckling. The upper and lower atomic layers are presented in blue and green colors, respectively. The buckling height $h$ is defined by the distance between the atoms within the same ML. (b) The $h$-dependent energy gap ($\Delta$) at Dirac point of $\alpha$-Bi ML. (c) Band structures of non-buckled ($h = 0$) $\alpha$-Bi without and with SOC as well as buckled $\alpha$-Bi with SOC at different buckling heights ($h = 0.1$ Å and 0.5 Å).[73]

### 3.2. The $\beta$ phase monolayer

Bismuth ML in $\beta$ phase has attracted attention immediately after the discovery of graphene due to the similar honeycomb structure. Bismuth is the heaviest group-V element and actually, it is also the heaviest element in periodic table without radioactivity. So, it possesses large SOC effect and is the most promising candidate to achieve 2D QSH phase. In 2006, $\beta$-Bi ML had been predicted to be topologically non-trivial with protected edge states[83] and the non-trivial gap is large enough for experimental measurement. Several experimental works provide evidences of the topological edge states in $\beta$-Bi ML as shown in Fig. 7, where the $dI/dV$ mapping shows the conducting states at the edges[84] and the STS profile crossing the edge shows a Dirac-point-like signal.[3,4]

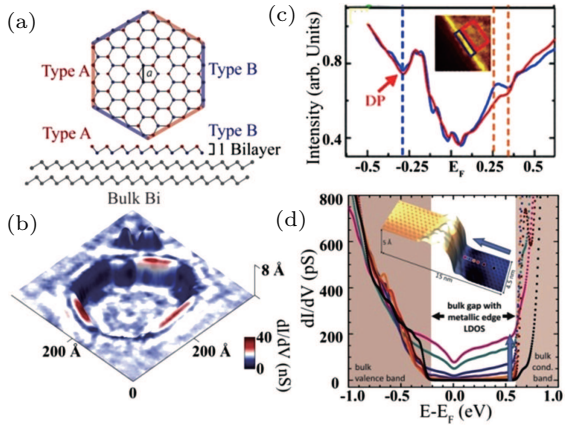



**Fig. 7.** (a) Crystal structure of $\beta$-Bi. Red and blue colors label the upper and lower atomic layers of the topmost bilayer, respectively. Here, bilayer means two (upper and lower) atomic layers. (b) Topography around the hexagonal pit-like defect, differential conductance is shown with color plot, showing high conductance at alternative edges.[89] (c) STS of the step edge (blue) and the inner terrace (red) of Bi/$Bi_2Te_3$ island averaged over the area as marked in the inset of (c). The STS, the bands aligned Dirac point "DP" as indicated by the blue dashed line. The orange dashed lines mark the band gap of the topmost Bi layer.[3] (d) Differential conductivity $dI/dV$ at different distances from the edge. A large gap of $\sim 0.8$ eV is observed in bulk bismuthene (black curve). Inset shows the STS measurement locations at uphill substrate step causing the boundary.[4]

The $\beta$-Sb and $\beta$-As in ground state are trivial insulators. However, they can sustain large tensile strain (e.g., 18.4% for As[85] and 18% for Sb[86]) that assists the topological phase transition. It was proposed that the topological phase transition from normal insulator to 2D QSH insulator occurs under biaxial strain of 11.7% and 14.5% for Sb and As, respectively.[85,86] This large strain may be achieved by some substrate as buffer layer during epitaxial growth. As the second heaviest element of group-V, $\beta$-Sb could become 2D TI by other ways. It was predicted that $\beta$-Sb becomes 2D TI when the thickness increases between 4 ML and 7 ML, where the surface band splitting provides a robust QSH gap at room temperature.[87] With further increased film thickness, a crossover from the 2D TI to the 3D TI occurs.[87] On the other hand, coupling with substrate could also cause

the topological phase transition in $\beta$-Sb and most recently, an experimental evidence of nontrivial topological edge states has been observed in epitaxially grown 2D $\beta$-Sb islands on copper Cu (111) substrate,[72] where the topological gap lies $\sim$ 1.5 eV above the Fermi level (Fig. 8). Similarly, $\beta$-P was also predicted to be a large indirect bandgap semiconductor ($>$ 2 eV),[58] and it has been proposed to be topologically non-trivial under 16% tensile strain.[88]

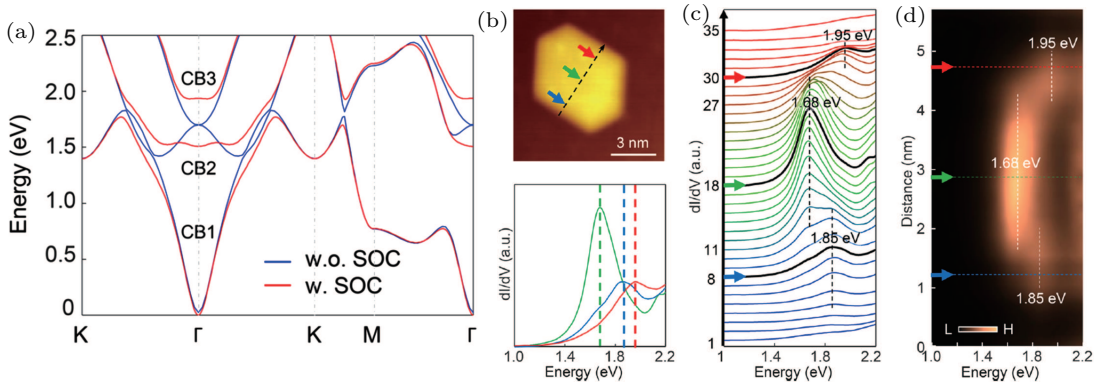



**Fig. 8.** Band structure of freestanding ($\beta$ phase) antimonene ML with and without SOC, represented by red and blue lines, respectively. (b) STM topography of a hexagonal honeycomb shaped antimonene island. The lower panel shows three d$I$/d$V$ curves measured at the edges and center of the island marked by blue, green, and red arrows in the upper panel. (c) Plot of spatially resolved data of 35 d$I$/d$V$ curves along the black dashed arrow in panel (b). The three d$I$/d$V$ curves marked by arrows correspond to those shown in panel (d) with peaks at 1.68 eV (green), 1.85 eV (blue), and 1.95 eV (red). (d) The intensity plot of the d$I$/d$V$ curves shown in panel (c).[72]

In general, crystal defects are really important for semiconductors, which could introduce additional defect states in bandgap affecting the transport properties. For topological materials, these defect states in bulk could introduce additional conducting states overcoming the advantage of the protected boundary states within bandgap. In comparison with compound systems, elemental systems are better with less defect problems, which is very important for the application of topological materials. This is one reason that researchers struggle to realize topological character in elemental systems. Recently, due to rising interest in QSH effect in group-V elemental MLs, 2D honeycomb structures of group-V binary compounds have also gained much attention,[90] e.g., SbAs, BiP, BiAs, BiSb, AsP, and SbP. Because all elements are group-V elements with isovalent electrons, there is no additional state appearing in the bandgap and the gap size can be tuned by applying a lattice strain. They all exhibit metal–indirect gap semiconductor–direct gap semiconductor–TI transitions under strain.[91] This broadens the potential candidates of 2D TIs in hexagonal $\beta$ phase of group-V elements.

### 3.3. Chemical functionalization of group-V MLs

Chemical functionalization is an important tool to control electronic properties of materials and oxidation process is easy for group-V elements. This could change the topological character and help the emergence of new topological states. For example, $\beta$-P ML (blue phosphorus) is a trivial insulator with large bandgap. This gap size decreases largely after oxidation ($P_2O_2$) due to the saturation of the lone pair electrons. And, a moderate strain can easily tune the three bands around the Fermi energy, resulting in tunable quantum phase transition between pseudospin-1 fermions and 2D double Weyl fermions (Figs. 9(a)–9(c)).[92,93] $\beta$-As ML also becomes a topological insulator exhibiting the quantum spin Hall effect when surface functionalized with H, F, OH, and $CH_3$ chemical group.[94,95]

Hydrogenation or halogenation is another effective method to introduce topological phase transition in group-V MLs. Here, we firstly discuss the functionalized $\beta$ phases. After functionalization, $Bi_2X_2$ or $Sb_2X_2$ ($X$ = H, F, Cl, Br) were predicted to be topologically non-trivial insulators and stable above room temperature (Figs. 9(d) and 9(e)).[96] These features make $Bi_2X_2$ (or $Sb_2X_2$) an ideal platform for the realization of many striking quantum phenomena at room temperature. Similarly, halogen functionalized $As_2X_2$ also opens up a large non-trivial gap, signifying its potential for future applications as high-speed devices. Furthermore, if functionalized 2D TI is grown on the magnetic substrate, the quantum anomalous Hall insulator may be achieved, e.g., $Sb_2H_2$ on antiferromagnetic substrate $LaFeO_3$ (111).[97] For the $\alpha$ phase of group-V, it is predicted that halogen-decorating on one side of MLs would generate a Dirac nodal line around the Fermi energy without SOC or hourglass fermions protected by nonsymmorphic symmetry when considering the SOC.[98]

As both $\alpha$ and $\beta$ phases of group-V MLs have one lone pair of electrons, functionalization by monovalence chemical groups is normally preferred to maintain chemical stability with tunable electronic structures. Although chemical functionalization is a good way to change the electronic structure of 2D materials including the topological properties of 2D group-V MLs, this functionalization is permanent with fixed change of electronic structure. It is hard to reversibly tune the electronic structure by chemical reaction which mostly evolves irreversible bond formation. It is more desirable for device application to change or switch the electronic character between two or more topological states reversibly.

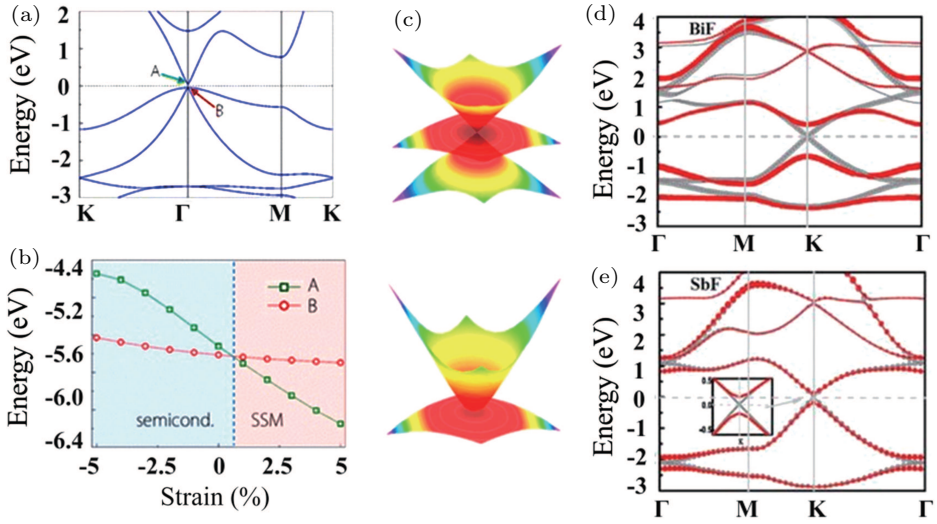



**Fig. 9.** (a) Electronic band structure of blue phosphorus oxide (BPO) without strain. A and B label the non-degenerate state at the conduction band bottom and the doubly-degenerate state at the valence band top, respectively. (b) Energies of A and B states versus strain. The crossing of the two corresponds to the quantum phase transition between a semiconductor phase and a symmetry protected semimetal (SSM) phase. (c) Energy dispersion around the band crossing point at Fermi level for critical strain +0.6% (upper panel) and (lower panel) +4% strain. The low-energy quasiparticles around the crossing point are described by 2D pseudospin-1 fermions and 2D double Weyl fermions.[92] Band structures of the (d) BiF and (e) SbF monolayers with (red) and without (gray) SOC. The bands around the Fermi level consist of the $p_x$ and $p_y$ orbitals. The size of the symbols is proportional to the population of the $p_x$ and $p_y$ orbitals.[96]

## 4. Ferroelectricity in 2D group-V materials

Ferroelectricity is a quantum order characterized by spontaneous alignment of electronic dipoles with switchable macroscopic electronic polarization. Ferroelectric materials with this switchable electrical polarization have attracted much research interest due to their applications in non-volatile memory devices, field effect transistors, sensors, solar cells, and so on.[37,38,99] Normally, ferroelectricity disappears when the film thickness is below a critical value because of the depolarizing electric field and electron screening. A new class of materials, called as hyperferroelectrics, has been identified, which can endure stable polar states in ultrathin atomic layers against unscreened depolarizing field.[39] This requires instability of a longitudinal optical mode in addition to the transverse-optical-mode instability of normal ferroelectrics. However, there is still lack of solid experimental evidence of these materials. Recently, the ferroelectric instability becomes of interest in 2D van der Waals materials. A lot of atomically thin ferroelectric materials have been predicted and experimentally realized in 2D van der Waals materials[100–102] and readers may refer to two recent topic review papers.[41,46] Such depolarization field effect in a true 2D system may no longer be an issue. Moreover, ferroelectric transition driven by electric field is even observed in 2D semimetals,[103,104] expanding our understanding of ferroelectricity.[105] These results show again that dimensionality makes major impact on materials properties and underlying physics.

### 4.1. The $\alpha$ phase monolayer

By scanning tunneling microscope and transport measurement, the 2D ferroelectricity has been confirmed in group-IV monochalcogenides, SnTe ML, which has puckered atomic structure.[100] The key condition of this ferroelectricity is the resonance bonding between cations and anions composing the puckered structure.[106] After that, ferroelectricity has been identified in a lot of 2D systems by replacing elements with isoconvalent state as SnTe, e.g., $MX$ ($M$ = Ge, Sn; $X$ = S, Se).[45] The $\alpha$ phase of 2D group-V elemental MLs has similar structure and the same valence electrons with 2D group-IV monochalcogenides. Thus, they are also possible to present ferroelectricity in puckered $\alpha$ phase.

Ferroelectricity has been mostly observed in compounds of different elements rather than elemental materials. The appearance of FE in elemental materials does not contradict the requirement of broken inversion symmetry. The major obstacle is that most nonmetallic elemental materials are stabilized in nonpolar structures of high symmetry, which prevents the electric polarization. This obstacle could be overcome in 2D system. As mentioned above, the atomic buckling in $\alpha$ phase breaks the inversion symmetry and very recently, Xiao *et al.* predicted the existence of FE in buckled $\alpha$-As, $\alpha$-Sb, and $\alpha$-Bi elemental MLs for the first time, as shown in Figs. 10(a)–10(c).[43] The spontaneous polarization in these buckled MLs is along the in-plane $x$-axis with a predicted high Curie temperature, which makes them promising candidates for ferroelectric devices. Further analysis of the free-energy contour and phonon spectrum confirmed that beyond the two FE phases (A and A′), there also exist anti-ferroelectric (AFE) metastable phases (C and C′) (Figs. 10(d) and 10(e)).

Compared with the 2D FE group-IV monochalcogenide materials, besides the fundamental distinction (compound vs. elemental), the mechanisms for the ferroelectric polariza-

tion of 2D group-V MLs are also different. The group-IV monochalcogenide materials break the centrosymmetry via in-plane distortion from the cubic structure as well as the occupation of lattice sites with different kinds of elements. In comparison, the group-V MLs break centrosymmetry by the out-of-plane atomic-layer buckling, whereas the in-plane distortion does not break the symmetry. As a result, the transformation between two degenerate FE structures of group-IV monochalcogenide materials requires the breaking and reforming bonds between atoms. This is the reason that the resonance bonding between atoms is important and required for the generation of ferroelectronic polarization in group-IV monochalcogenide compounds.[106] Whereas for the group-V monolayers, there is no significant bonding and bond-breaking character in the transformation between two degenerate FE structures. Moreover, the puckered structure of the elemental MLs permits the presence of an AFE phase (for $\alpha$-Bi), which is absent in the compound materials. The coexistence of FE and AFE phases in the same materials is important. As the symmetry and geometrical structure of AFE phase are different from those of FE phase, its electronic structures could be largely changed in topological nature. This interplay between geometrical phase transition and electronic polarization allows an extraordinary control of the electronic structure (e.g., electronic topological properties) via external field. In addition, the electronic polarization is sensitive to buckling height $h$ and interaction with the substrate, giving us more freedom to engineer the electronic structures and phase transition of the van der Waals heterostructure devices based on group-V elemental MLs.

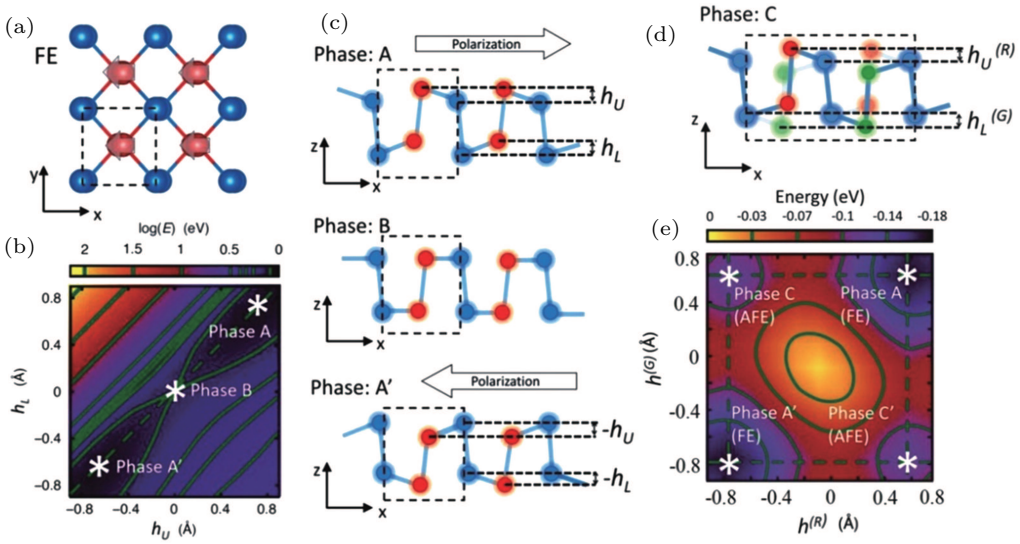



**Fig. 10.** (a) Top view of $\alpha$ phase group-V elemental ML. The unit cell is indicated with black dashed rectangle lines. (b) Free energy contour for $\alpha$-As ML versus the buckling heights ($h_U$, $h_L$). The phases A, A′, and B are marked. (c) Side views of the two energy-degenerate distorted noncentrosymmetric structures (A and A′ phases) and undistorted centrosymmetric structure (phase B). The height differences between upper (red) and lower (blue) atomic layers are marked as $h_U$ and $h_L$, respectively. (d) Side view of $\alpha$-Bi ML in antiferroelectric (AFE) configuration. The atomic sites shifted up and down are colored in red and green, respectively. (e) Free energy contour of Bi MLs versus buckling heights ($h^{(R)}$, $h^{(G)}$). For Bi, besides the FE phases A and A′, there also exist metastable AFE phases C and C′.[43]

It has also been predicted that 2D group-V binary compounds composed of both light and heavy group-V elements present ferroelectricity in $\alpha$ or $\gamma$ phase with notable large and strain tunable spontaneous polarization, e.g., BiN,[107] SbN, BiP.[108] SbP, and SbAs.[109] Such large polarization is caused by the immense electronegativity difference of the light and heavy group-V elements and their displacement in the polarization plane. The mechanism for the ferroelectric transition is almost the same as that of 2D group-IV monochalcogenide compounds requiring the breaking and reforming bonds between atoms. In addition, ferroelectricity is also predicted in halogen-intercalated $\alpha$-P bilayer without buckling, where the ferroelectric transition is determined by the shift of the halogen atoms covalently bonded to up-layer or down-layer.[110] This concept may be extended to other van der Waals bilayers, but it is really challenging in experiment to precisely functionalize the target material to control these quantum orders.

### 4.2. The $\beta$ phase monolayer

In hexagonal honeycomb $\beta$ phase, the out-of-plane atomic-layer buckling does not break the inversion symmetry and the group-V elemental MLs remain centrosymmetric without ferroelectricity no matter whether they are planar or buckled 2D layers. One possible way to break centrosymmetry is to fabricate AB binary monolayer with a bipartite corrugated honeycomb lattice, where the A and B atoms are different elements. Binary group-V compounds show a spontaneous FE polarization in freestanding buckled $\beta$ phase and their polarization is switched by changing the relative position of the two atoms along out-of-plane direction. The presence of a diatomic basis that breaks the inversion symmetry even in the planar geometry leads to the emergence of Zeeman-

like spin-split bands with coupled spin-valley physics analogous to the $MoS_2$ case.[111] Meanwhile, it is mainly responsible for the onset of the FE phase when the honeycomb lattice buckles, allowing for an electrically controllable Rashba-like spin-texture around the valleys, whose chirality is locked to the polarization direction and therefore fully reversible upon FE switching.[42] These spin split bands can be effectively detected by spin-resolved spectroscopic techniques and binary $\beta$ phase compounds allow for the engineering of 2D spin field-effect-transistors.[112]

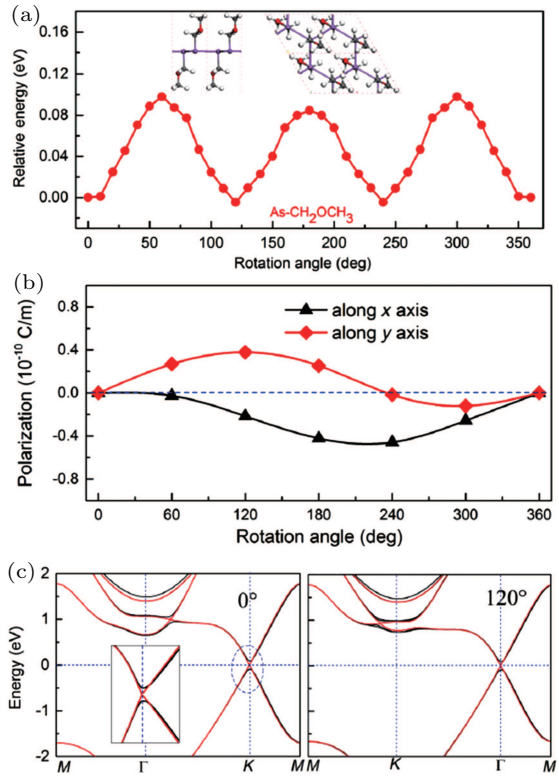



**Fig. 11.** (a) Energy variation and kinetic barrier for $CH_2OCH_3$ rotations in functionalized arsenene; the insets show the structural models. (b) Variation of the polarization along the $x$ and $y$ directions. (c) Electronic band structures of the symmetric ligand configuration with the rotation angle of 0° (left) and the the asymmetric ligand configuration with the rotation angle of 120° (right). The topological order is preserved under the ligand rotation, although there is a band splitting due to an out-of-plane symmetry breaking.[113]

Chemical functionalization of polar chemical group is another direct and possible way to transform centrosymmetric $\beta$ phase into polar structure. It is proposed that ferroelectricity can be introduced into $\beta$-As ML by passivation of $CH_2OCH_3$ ligand.[90] The fully relaxed structure of $CH_2OCH_3$ functionalized $\beta$-As is shown in the inset of Fig. 11(a), where arsenene is flat without any out-of-plane buckling and remains centrosymmetry. When $CH_2OCH_3$ is adsorbed on $\beta$-As ML, it becomes polarized with local dipole. The in-plane electronic polarization is achieved by ligand molecules alignment and a ferroelectric transition can be driven by a ligand rotation mechanism (Fig. 11(b)). Actually, this concept can date back to an early work[114] and is expected to be a more general phenomenon in 2D-layered materials. Similar to $\beta$-As passivated by simple ligands as mentioned before, $CH_2OCH_3$-functionalized $\beta$-As becomes a topologically nontrivial insulator with QSH effect. The electronic structure and topological character are mainly determined by the bonding between $\beta$-As and ligand, not the relative position or rotation of $CH_2OCH_3$ sitting on top of the As atoms. Thus, the topological phase and nontrivial band gap are robust and well preserved when ligand $CH_2OCH_3$ molecules are rotated (Fig. 11(c)) without interplay between the topological character and ferroelectricity. On the other hand, the total energies of multiple rotated configurations with different polarizations are quite close to each other, which means that the ligand molecules may not be orderly arranged as shown in Fig. 11(a). However, this controllable in-plane ferroelectricity maybe has wide applications in memory or logical device designs and the storage density can be quite high as the information bit can be directly related to one ligand arrangement.

## 5. Relationship of FE and TI

As both ferroelectricity and electronic topological character are closely linked to the geometrical symmetry and structural distortion, the interplay between them can be mediated by geometrical distortion and their coexistence could enable precise control of electronic topology using electric fields (determined by geometrical distortion in phase transition), enhancing the applicability of topological materials in electronics and spintronics. Unfortunately, the crystal structure of 3D group-V is the centrosymmetric one without electronic polarization. Very recently, it is found that both electronic polarization and nontrivial topology can coexist in some compounds containing group-V elements.[115–117] An extremely rich physics strongly links to the ferroelectric properties, ranging from electric control of bulk Rashba effect to the transitions among a 3D topological insulator, normal insulator, and Weyl semimetals. It is also proposed to realize topologically protected Weyl semimetal and nodal line semimetal phases in IV–VI semiconducting compounds (isovalent as group-V in average) with the low-temperature ferroelectric phase.[118,119] These pave a way to explore the coupling between topological properties and electronic polarization in low dimensional systems.

There is more freedom allowing crystal-symmetry variation and distortion in 2D group-V MLs, which is important for the emergence of multiple quantum ordering. In puckered $\alpha$ phase, out-of-plane atomic-layer buckling is flexible and can vary in a wide range. This buckling breaks centrosymmetry and also changes the electronic topological character. For $\alpha$-Bi, it is an intrinsic 2D TI with QSH effect when the buckling is zero. This corresponds to a paraelectric state. When the buckling is strong and large ($> 0.1$ Å), $\alpha$-Bi becomes a normal insulator without centrosymmetry and corresponds to a

ferroelectric state. Thus, the topological phase transition with and without topological protected boundary states may be controlled by the ferro–paraelectric phase transition through geometrical distortion. It is interesting that when the buckling is weak ($< 0.1$ Å) under strain, the QSH effect is persisted and coexists with FE in this single phase material. As there are two ferroelectric states with opposite polarizations and they are related to each other via an inversion operation, the chirality and direction of the spin-locked current at boundary rely on the direction of the ferroelectric polarization, as shown in Figs. 12(a) and 12(c). Thus, it may promote novel applications in conceptually new devices, where the direction of spin current is fully controlled by ferroelectricity. Since the direction of spin-locked current can be viewed as a ferroic order, this is some kind of multiferroics.

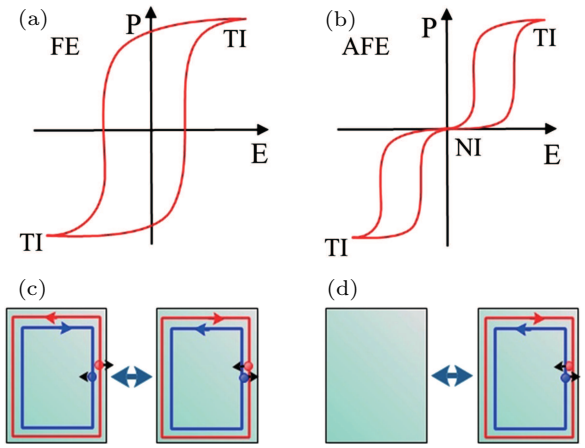



**Fig. 12.** Schematic representation of ferroelectric topological insulators (a) with two polar states and (b) with two polar TI states and an antipolar normal insulator (NI) state. (c) Proposed switching device corresponding to the two polar TI states with ferroelectric polarization. (d) Switching boundary conductivity on/off of an antipolar NI and two polar TI states. The chirality of electronic current is labeled by red and blue lines respectively. The up and down spins are indicated by short black arrows on the lines.

One the other hand, AFE could coexist with FE in 2D group-V elemental ML. The crystal symmetry and distortion of AFE are distinctly different from those of FE, resulting in different electronic structure and topological character. For example, AFE and FE states may correspond to an antipolar normal insulator (NI) state and two polar topological insulator (TI) states, respectively, as shown in Fig. 12(b). There is no protected boundary state within the bandgap of NI, while the dissipationless boundary states are expected at the edges of TI which are protected by the topological nature. It could enable precise control of topology and switching on/off the topological boundary states using electric fields (Fig. 12(d)), enhancing the applicability of topological materials in electronics and spintronics.

## 6. Perspective

The recent progress in QSH insulators, 2D ferroelectricity, and experimental fabrication of group-V elemental MLs has motivated the researchers to revisit group-V materials. They are potential candidates for realization of 2D TIs and their topological properties can be controlled by electric field, strain, substrate effect, or chemical functionalization. Recent experimental evidences of non-trivial topology in 2D Bi and Sb have robustly boosted the research interest. Moreover, group-V MLs are the first predicted ferroelectric elemental materials in 2D limit, which violate the traditional concept and broaden the 2D ferroelectric family.

Ferroelectricity and QSH effect are two intriguing quantum phenomena in modern condensed matter physics and both of them are related to the integration of Berry phase in BZ. The co-existing QSH effect and ferroelectricity in the same material may lead to novel physical properties, e.g., topological magneto-electric effect.[120] The effective integration of these two properties is not only important for the novel applications in devices, but also leads to the discoveries of unusual quantum phenomena, e.g., the formation of quantum Hall ferroelectric states[121,122] and nonlinear Hall effect.[123,124] In addition, as 2D materials, they can easily grow or deposit on substrates with other quantum properties. Actually, it has been confirmed in experiment that superconductivity can be introduced into 2D Bi ML by deposition on a superconducting substrate due to the superconductor proximity effect.[125] Therefore, 2D group-V MLs provide a good platform to study the interplay between multiple quantum properties.

## References

[1] Liu C C, Feng W and Yao Y 2011 *Phys. Rev. Lett.* **107** 076802
[2] Sheng D N, Weng Z Y, Sheng L and Haldane F D M 2006 *Phys. Rev. Lett.* **97** 036808
[3] Murakami S 2006 *Phys. Rev. Lett.* **97** 236805
[4] Reis F, Li G, Dudy L, Bauernfeind M, Glass S, Hanke W and Thomale R 2017 *Science* **357** 287
[5] Wu M, Dong S, Yao K, Liu J and Zeng X C 2016 *Nano Lett.* **16** 7309
[6] Baskaran G 2018 *Many-body Approaches at Different Scales: A Tribute to Norman H. March on the Occasion of his* 90*th Birthday* (Angilella G G N and Amovilli C, Ed.) (Cham: Springer International Publishing) p. 43
[7] Liao M, Zang Y, Guan Z, Li H, Gong Y, Zhu K, Hu X P, Zhang D, Xu Y, Wang Y Y, He K, Ma X C, Zhang S C and Xue Q K 2018 *Nat. Phys.* **14** 344
[8] Xing Y, Fu H L, Liu H, Sun Y, Wang F, Lin X, Wang J, Zhang H M, Peng J P, Ma X C and Xue Q K 2015 *Science* **350** 542
[9] Gibertini M, Koperski M, Morpurgo A F and Novoselov K S 2019 *Nat. Nanotechnol.* **14** 408
[10] Gong C, Li L, Li Z, Ji H, Stern A, Xia Y, Cao T, Bao W, Wang C, Wang Y, Qiu Z Q, Cava R J, Louie S G, Xia J and Zhang X 2017 *Nature* **546** 265
[11] Huang B, Clark G, Navarro-Moratalla E, Klein D R, Cheng R, Seyler K L, Zhong D, Schmidgall E, McGuire M A, Cobden D H, Yao W, Xiao D, Jarillo-Herrero P and Xu X 2017 *Nature* **546** 270
[12] Novoselov K S, Geim A K, Morozov S V, Jiang D, Katsnelson M I, Grigorieva I V, Dubonos S V and Firsov A A 2005 *Nature* **438** 197
[13] Geim A K and Novoselov K S 2007 *Nat. Mater.* **6** 183
[14] Feng B, Ding Z, Meng S, Yao Y, He X, Cheng P, Chen L and Wu K 2012 *Nano Lett.* **12** 3507
[15] Fleurence A, Friedlein R, Ozaki T, Kawai H, Wang Y and Yamada-Takamura Y 2012 *Phys. Rev. Lett.* **108** 245501
[16] Vogt P, De Padova P, Quaresima C, Avila J, Frantzeskakis E, Asensio M C, Resta A, Ealet B and Le Lay G 2012 *Phys. Rev. Lett.* **108** 155501

[17] Li L, Lu S Z, Pan J, Qin Z, Wang Y Q, Wang Y, Cao G Y, Du S and Gao H J 2014 *Adv. Mater.* **26** 4820
[18] Zhang L, Bampoulis P, Rudenko A N, Yao Q, Van Houselt A, Poelsema B, Katsnelson M I and Zandvliet H J W 2016 *Phys. Rev. Lett.* **116** 256804
[19] Zhu F, Chen W, Xu Y, Gao C, Guan D, Liu C, Qian D, Zhang S C and Jia J 2015 *Nat. Mater.* **14** 1020
[20] Li W, Kong L, Chen C, Gou J, Sheng S, Zhang W, Li H, Chen L, Cheng P and Wu K 2018 *Sci. Bull.* **63** 282
[21] Li L, Yu Y, Ye G J, Ge Q, Ou X, Wu H, Feng D, Chen X H and Zhang Y 2014 *Nat. Nanotechnol.* **9** 372
[22] Vishnoi P, Mazumder M, Pati S K and R Rao C N 2018 *New J. Chem.* **42** 14091
[23] Shao Y, Liu Z L, Cheng C, Wu X, Liu H, Liu C, Wang J O, Zhu S Y, Wang Y Q, Shi D X, Ibrahim K, Sun J T, Wang Y L and Gao H J 2018 *Nano Lett.* **18** 2133
[24] Huang X, Guan J, Lin Z, Liu B, Xing S, Wang W and Guo J 2017 *Nano Lett.* **17** 4619
[25] Qin J, Qiu G, Jian J, Zhou H, Yang L, Charnas A, Zemlyanov D Y, Xu C Y, Xu X, Wu W, Wang H and Ye P D 2017 *ACS Nano* **11** 10222
[26] Kane C L and Mele E J 2005 *Phys. Rev. Lett.* **95** 226801
[27] Chen Y L, Analytis J G, Chu J H, Liu Z K, Mo S K, Qi X L, Zhang H J, Lu D H, Dai X, Fang Z, Zhang S C, Fisher I R, Hussain Z and Shen Z X 2009 *Science* **325** 178
[28] Hsieh D, Xia Y, Qian D, Wray L, Meier F, Dil J H, Osterwalder J, Patthey L, Fedorov A V, Lin H, Bansil A, Grauer D, Hor Y S, Cava R J and Hasan M Z 2009 *Phys. Rev. Lett.* **103** 146401
[29] Qi X L and Zhang S C 2011 *Rev. Mod. Phys.* **83** 1057
[30] Zhang S, Zhu W and Sun Q 2013 *J. Phys. Condens. Matter* **25** 295301
[31] Yao Y, Ye F, Qi X L, Zhang S C and Fang Z 2007 *Phys. Rev. B* **75** 041401
[32] Xu Y, Yan B, Zhang H J, Wang J, Xu G, Tang P, Duan W and Zhang S C 2013 *Phys. Rev. Lett.* **111** 136804
[33] Cahangirov S, Topsakal M, Aktürk E, Şahin H and Ciraci S 2009 *Phys. Rev. Lett.* **102** 236804
[34] Vishnoi P, Pramoda K and Rao C N R 2019 *ChemNanoMat* **5** 1062
[35] Auciello O, Scott J F and Ramesh R 1998 *Phys. Today* **51** 22
[36] Nuraje N and Su K 2013 *Nanoscale* **5** 8752
[37] Dawber M, Rabe K M and Scott J F 2005 *Rev. Mod. Phys.* **77** 1083
[38] Scott J F 2007 *Science* **315** 954
[39] Garrity K F, Rabe K M and Vanderbilt D 2014 *Phys. Rev. Lett.* **112** 127601
[40] Wu M and Jena P 2018 *Wiley Interdiscip. Rev. Comput. Mol. Sci.* **8** e1365
[41] Guan Z, Hu H, Shen X, Xiang P, Zhong N, Chu J and Duan C 2020 *Adv. Electron. Mater.* **6** 1900818
[42] Di Sante D, Stroppa A, Barone P, Whangbo M H and Picozzi S 2015 *Phys. Rev. B* **91** 161401
[43] Xiao C, Wang F, Yang S A, Lu Y, Feng Y and Zhang S 2018 *Adv. Funct. Mater.* **28** 1707383
[44] Wu M and Zeng X C 2016 *Nano Lett.* **16** 3236
[45] Fei R, Kang W and Yang L 2016 *Phys. Rev. Lett.* **117** 097601
[46] Lu C, Wu M, Lin L and Liu J M 2019 *Natl. Sci. Rev.* **6** 653
[47] Liu J, Fang C and Fu L 2019 *Chin. Phys. B* **28** 047301
[48] Zhang L, Huang H, Zhang B, Gu M, Zhao D, Zhao X, Li L, Zhou J, Wu K, Cheng Y and Zhang J 2019 *Angew. Chem. Int. Ed.* **58** 1074
[49] Brown A and Rundqvist S 1965 *Acta Crystallogr.* **19** 684
[50] Bridgman P W 1914 *J. Am. Chem. Soc.* **36** 1344
[51] Hultgren R, Gingrich N S and Warren B E 1935 *J. Chem. Phys.* **3** 351
[52] Ruck M, Hoppe D, Wahl B, Simon P, Wang Y and Seifert G 2005 *Angew. Chem. Int. Ed.* **44** 7616
[53] Jacobs R B 1937 *J. Chem. Phys.* **5** 945
[54] Jamieson J C 1963 *Science* **139** 1291
[55] Saito M, Takemori Y, Hashi T, Nagao T and Yaginuma S 2007 *Jpn. J. Appl. Phys.* **46** 7824
[56] Namari N A P and Saito M 2019 *Jpn. J. Appl. Phys.* **58** 061003
[57] Burford N, Carpenter Y Y, Conrad E and Saunders C D L 2010 *Biol. Chem. Arsenic Antimony Bismuth* **1**
[58] Zhu Z and Tománek D 2014 *Phys. Rev. Lett.* **112** 176802
[59] Zhang S, Xie M, Li F, Yan Z, Li Y, Kan E, Liu W, Chen Z and Zeng H 2016 *Angew. Chem. Int. Ed.* **55** 1666
[60] Wu M, Fu H, Zhou L, Yao K and Zeng X C 2015 *Nano Lett.* **15** 3557
[61] Zhuo Z, Wu X and Yang J 2016 *J. Am. Chem. Soc.* **138** 7091
[62] Liu H, Neal A T, Zhu Z, Luo Z, Xu X, Tománek D and Ye P D 2014 *ACS Nano* **8** 4033
[63] Zhang J L, Zhao S, Han C, Wang Z, Zhong S, Sun S, Guo R, Zhou X, Gu C D, Di K, Li Z and Chen W 2016 *Nano Lett.* **16** 4903
[64] Gibaja C, Rodriguez-San-Miguel D, Ares P, Gómez-Herrero J, Varela M, Gillen R, Maultzsch J, Hauke F, Hirsch A, Abellán G and Zamora F 2016 *Angew. Chem. Int. Ed.* **55** 14345
[65] Yang Z, Wu Z, Lyu Y and Hao J 2019 *InfoMat* **1** 98
[66] Shi Z Q, Li H, Yuan Q Q, Song Y H, Lv Y Y, Shi W, Jia Z Y, Gao L, Chen Y B, Zhu W and Li S C 2019 *Adv. Mater.* **31** 1806130
[67] Yuhara J, Fujii Y, Nishino K, Isobe N, Nakatake M, Xian L, Rubio A and Le Lay G 2018 *2D Mater.* **5** 025002
[68] Nagao T, Sadowski J, Saito M, Yaginuma S, Fujikawa Y, Kogure T, Ohno T, Hasegawa Y, Hasegawa S and Sakurai T 2004 *Phys. Rev. Lett.* **93** 105501
[69] Xu J P, Zhang J Q, Tian H, Xu H, Ho W and Xie M 2017 *Phys. Rev. Mater.* **1** 061002
[70] Zhuang J, Liu C, Gao Q, Liu Y, Feng H, Xu X, Wang J, Zhao J, Dou S X, Hu Z and Du Y 2018 *ACS Nano* **12** 5059
[71] Lu W, Nan H, Hong J, Chen Y, Zhu C, Liang Z, Ma X, Ni Z, Jin C and Zhang Z 2014 *Nano Res.* **7** 853
[72] Zhu S Y, Shao Y, Wang E, Cao L, Li X Y, Liu Z L, Liu C, Liu L W, Wang J O, Ibrahim K, Sun J T, Wang Y L, Du S and Gao H J 2019 *Nano Lett.* **19** 6323
[73] Lu Y, Xu W, Zeng M, Yao G, Shen L, Yang M, Luo Z, Pan F, Wu K, Das T, He P, Jiang J, Martin J, Feng Y P, Lin H and Wang X 2015 *Nano Lett.* **15** 80
[74] Zhang S, Guo S, Chen Z, Wang Y, Gao H, Gómez-Herrero J, Ares P, Zamora F, Zhu Z and Zeng H 2018 *Chem. Soc. Rev.* **47** 982
[75] Hasan M Z and Kane C L 2010 *Rev. Mod. Phys.* **82** 3045
[76] Dai X, Le C C, Wu X X, Qin S S, Lin Z P and Hu J P 2016 *Chin. Phys. Lett.* **33** 127301
[77] Fu L and Kane C L 2007 *Phys. Rev. B* **76** 045302
[78] Lu Y, Zhou D, Chang G, Guan S, Chen W, Jiang Y, Jiang J, Wang X, Yang S A, Feng Y P, Kawazoe Y and Lin H 2016 *npj Comput. Mater.* **2** 16011
[79] Kamal C and Ezawa M 2015 *Phys. Rev. B* **91** 085423
[80] Liu Q, Zhang X, Abdalla L B, Fazzio A and Zunger A 2015 *Nano Lett.* **15** 1222
[81] Kim J, Baik S S, Ryu S H, Sohn Y, Park S, Park B G, Denlinger J, Yi Y, Choi H J and Kim K S 2015 *Science* **349** 723
[82] Märkl T, Kowalczyk P J, Le Ster M, Mahajan I V, Pirie H, Ahmed Z, Bian G, Wang X, Chiang T C and Brown S A 2017 *2D Mater.* **5** 011002
[83] Hirahara T, Nagao T, Matsuda I, Bihlmayer G, Chulkov E V, Koroteev Y M, Echenique P M, Saito M and Hasegawa S 2006 *Phys. Rev. Lett.* **97** 146803
[84] Drozdov I K, Alexandradinata A, Jeon S, Nadj-Perge S, Ji H, Cava R J, Andrei Bernevig B and Yazdani A 2014 *Nat. Phys.* **10** 664
[85] Zhang H, Ma Y and Chen Z 2015 *Nanoscale* **7** 19152
[86] Zhao M, Zhang X and Li L 2015 *Sci. Rep.* **5** 16108
[87] Zhang P, Liu Z, Duan W, Liu F and Wu J 2012 *Phys. Rev. B* **85** 201410
[88] Yang G, Xu Z, Liu Z, Jin S, Zhang H and Ding Z 2017 *J. Phys. Chem. C* **121** 12945
[89] Drozdov I K, Alexandradinata A, Jeon S, Nadj-Perge S, Ji H, Cava R J, Bernevig B A and Yazdani A 2014 arXiv:14042598v1[cond-mat.mes-hall]
[90] Guo S, Zhang Y, Ge Y, Zhang S, Zeng H and Zhang H 2019 *Adv. Mater.* **31** 1902352
[91] Nie Y, Rahman M, Wang D, Wang C and Guo G 2016 *Sci. Rep.* **5** 17980
[92] Zhu L, Wang S S, Guan S, Liu Y, Zhang T, Chen G and Yang S A 2016 *Nano Lett.* **16** 6548
[93] Hua C, Li S, Xu Z, Zheng Y, Yang S A and Lu Y 2020 *Adv. Sci.* **7** 1901939
[94] Zhao J, Li Y and Ma J 2016 *Nanoscale* **8** 9657
[95] Wang Y, Ji W, Zhang C, Li P, Li F, Ren M, Chen X L, Yuan M and Wang P 2016 *Sci. Rep.* **6** 20342
[96] Song Z, Liu C C, Yang J, Han J, Ye M, Fu B, Yang Y, Niu Q, Lu J and Yao Y 2014 *NPG Asia Mater.* **6** e147
[97] Zhou T, Zhang J, Xue Y, Zhao B, Zhang H, Jiang H and Yang Z 2016 *Phys. Rev. B* **94** 235449
[98] Jin K H, Huang H, Wang Z and Liu F 2019 *Nanoscale* **11** 7256

[99] Wang Y, Xiao C, Chen M, Hua C, Zou J, Wu C, Jiang J, Yang S A, Lu Y and Ji W 2018 *Mater. Horizons* **5** 521
[100] Chang K, Liu J, Lin H, Wang N, Zhao K, Zhang A, Jin F, Zhong Y, Hu X, Duan W, Zhang Q, Fu L, Xue Q K, Chen X and Ji S H 2016 *Science* **353** 274
[101] Liu F, You L, Seyler K L, Li X, Yu P, Lin J, Wang X, Zhou J, Wang H, He H, Pantelides S T, Zhou W, Sharma P, Xu X, Ajayan P M, Wang J and Liu Z 2016 *Nat. Commun.* **7** 12357
[102] Xiao J, Zhu H, Wang Y, Feng W, Hu Y, Dasgupta A, Han Y, Wang Y, Muller D A, Martin L W, Hu P and Zhang X 2018 *Phys. Rev. Lett.* **120** 227601
[103] Sharma P, Xiang F X, Shao D F, Zhang D, Tsymbal E Y, Hamilton A R and Seidel J 2019 *Sci. Adv.* **5** eaax5080
[104] Fei Z, Zhao W, Palomaki T A, Sun B, Miller M K, Zhao Z, Yan J, Xu X and Cobden D H 2018 *Nature* **560** 336
[105] Tu Z, Wu M and Zeng X C 2017 *J. Phys. Chem. Lett.* **8** 1973
[106] Kooi B J and Noheda B 2016 *Science* **353** 221
[107] Chen P, Zhang X J and Liu B G 2019 *ACS Appl. Nano Mater.* **2** 58
[108] Liu C, Wan W, Ma J, Guo W and Yao Y 2018 *Nanoscale* **10** 7984
[109] Shen S, Liu C, Ma Y, Huang B and Dai Y 2019 *Nanoscale* **11** 11864
[110] Yang Q, Xiong W, Zhu L, Gao G and Wu M 2017 *J. Am. Chem. Soc.* **139** 11506
[111] Xiao D, Liu G B, Feng W, Xu X and Yao W 2012 *Phys. Rev. Lett.* **108** 196802
[112] Di Sante D, Barone P, Bertacco R and Picozzi S 2013 *Adv. Mater.* **25** 509
[113] Kou L, Ma Y, Liao T, Du A and Chen C 2018 *Phys. Rev. Appl.* **10** 024043
[114] Wu M, Burton J D, Tsymbal E Y, Zeng X C and Jena P 2012 *J. Am. Chem. Soc.* **134** 14423
[115] Monserrat B, Bennett J W, Rabe K M and Vanderbilt D 2017 *Phys. Rev. Lett.* **119** 036802
[116] Di Sante D, Barone P, Stroppa A, Garrity K F, Vanderbilt D and Picozzi S 2016 *Phys. Rev. Lett.* **117** 076401
[117] He J, Di Sante D, Li R, Chen X Q, Rondinelli J M and Franchini C 2018 *Nat. Commun.* **9** 492
[118] Lau A and Ortix C 2019 *Phys. Rev. Lett.* **122** 186801
[119] Sun L and Wan S L 2015 *Chin. Phys. Lett.* **32** 057501
[120] Qi X, Li R, Zang J and Zhang S 2009 *Science* **323** 1143f
[121] Hu X, Pang Z, Zhang C, Wang P, Li P and Ji W 2019 *J. Mater. Chem. C* **7** 9406
[122] Kou L, Fu H, Ma Y, Yan B, Liao T, Du A and Chen C 2018 *Phys. Rev. B* **97** 075429
[123] Kang K, Li T, Sohn E, Shan J and Mak K F 2019 *Nat. Mater.* **18** 324
[124] Du Z Z, Wang C M, Li S, Lu H Z and Xie X C 2019 *Nat. Commun.* **10** 3047
[125] Sun H H, Wang M X, Zhu F, Wang G Y, Ma H Y, Xu Z A, Liao Q, Lu Y, Gao C L, Li Y Y, Liu C, Qian D, Guan D and Jia J F 2017 *Nano Lett.* **17** 3035